



Quantification and discriminative power of ^{18}F -FE-PE2I PET in patients with Parkinson's disease

Aline Delva^{1,2} · Donatienne Van Weehaeghe^{3,4} · June van Aalst⁴ · Jenny Ceccarini⁴ · Michel Koole⁴ · Kristof Baete^{3,4} · Johan Nuyts⁴ · Wim Vandenberghe^{1,2} · Koen Van Laere^{3,4}

Received: 15 July 2019 / Accepted: 17 October 2019 / Published online: 27 November 2019
© Springer-Verlag GmbH Germany, part of Springer Nature 2019

Abstract

Rationale Dopamine transporter (DAT) imaging is an important adjunct in the diagnostic workup of patients with Parkinsonism. ^{18}F -FE-PE2I is a suitable PET radioligand for DAT quantification and imaging with good pharmacokinetics. The aim of this study was to determine a clinical optimal simplified reference tissue-based image acquisition protocol and to compare the discriminatory value and effect size for ^{18}F -FE-PE2I to that for ^{123}I -FP-CIT scan currently used in clinical practice.

Methods Nine patients with early Parkinson's disease (PD, 64.3 ± 6.8 years, 3M), who had previously undergone a ^{123}I -FP-CIT scan as part of their diagnostic workup, and 34 healthy volunteers (HV, 47.7 ± 16.8 years, 13M) underwent a 60-min dynamic ^{18}F -FE-PE2I PET-MR scan on a GE Signa 3T PET-MR. Based on dynamic data and MR-based VOI delineation, BP_{ND} , semi-quantitative uptake ratio and $\text{SUVR}_{[t_1-t_2]}$ images were calculated using either occipital cortex or cerebellum as reference region. For start-and-end time of the SUVR interval, three time frames $[t_1-t_2]$ were investigated: [15–40] min, [40–60] min, and [50–60] min postinjection. Data for putamen (PUT) and caudate nucleus-putamen ratio (CPR) were compared in terms of quantification bias versus BP_{ND} and discriminative power.

Results Using occipital cortex as reference region resulted in smaller bias of SUVR with respect to $\text{BP}_{\text{ND}} + 1$ and higher correlation between SUVR and $\text{BP}_{\text{ND}} + 1$ compared with using cerebellum, irrespective of SUVR $[t_1-t_2]$ interval. Smallest bias was observed with the [15–40]-min time window, in accordance with previous literature. The correlation between $\text{BP}_{\text{ND}} + 1$ and SUVR was slightly better for the late time windows. Discriminant analysis between PD and HV using both PUT and CPR SUVRs showed an accuracy of $\geq 90\%$, for both reference regions and all studied time windows. Semi-quantitative ^{123}I -FP-CIT and ^{18}F -FE-PE2I values and relative decrease in the striatum for patients were highly correlated, with a higher effect size for ^{18}F -FE-PE2I for PUT and CPR SUVR.

Conclusion ^{18}F -FE-PE2I is a suitable radioligand for in vivo DAT imaging with high discriminative power between early PD and healthy controls. Whereas a [15–40]-min window has lowest bias with respect to BP_{ND} , a [50–60]-min time window at pseudoequilibrium can be advocated in terms of clinical feasibility with optimal discriminative power. The occipital cortex may be slightly preferable as reference region because of the higher time stability, stronger correlation of SUVR with $\text{BP}_{\text{ND}} + 1$, and lower bias. Moreover, the data suggest that the diagnostic accuracy of a 10-min static ^{18}F -FE-PE2I scan is non-inferior compared with ^{123}I -FP-CIT scan used in standard clinical practice.

Keywords Parkinson's disease · DAT (dopamine transporter) · PET (positron emission tomography) · ^{18}F -FE-PE2I · ^{123}I -FP-CIT

Aline Delva and Donatienne Van Weehaeghe contributed equally to this work.

This article is part of the Topical Collection on Neurology

✉ Aline Delva
aline.delva@kuleuven.be

¹ Department of Neurosciences, KU Leuven, Leuven, Belgium

² Department of Neurology, University Hospitals Leuven, Herestraat 49, Leuven 3000, Belgium

³ Division of Nuclear Medicine, University Hospitals Leuven, Herestraat 49, Leuven 3000, Belgium

⁴ Nuclear Medicine and Molecular Imaging, Department of Imaging and Pathology, KU Leuven, Leuven, Belgium

Introduction

The dopamine transporter (DAT), a membrane protein expressed on the presynaptic terminals of nigrostriatal dopaminergic neurons, is important for dopamine reuptake from the synaptic cleft. Degeneration of nigrostriatal dopaminergic neurons is a hallmark of Parkinson's disease (PD) and is associated with progressive loss of dopamine transporters [1, 2]. PD affects 2–3% of population above the age of 65 years and is characterized by tremor, bradykinesia, rigidity, and a wide variety of non-motor symptoms [3]. DAT imaging plays a crucial role in the diagnostic workup of patients with clinically uncertain Parkinsonism as it allows in vivo assessment of dopaminergic system integrity [4].

Until now, DAT imaging in daily clinical practice is performed mainly using single photon emitting tracers such as ^{123}I -FP-CIT-SPECT (^{123}I N- ω -fluoropropyl-2 β -carbomethoxy-3 β -(4-iodophenyl)nortropine) [1, 5]. However, PET ligands allow better spatial resolution down to 3–4 mm [1, 5, 6]. Both ^{11}C and ^{18}F labeled PET radioligands bound to the nortropine analog PE2I have been investigated [7–10]. ^{18}F -FE-PE2I (^{18}F -(E)-N-(3-iodoprop-2-enyl)-2 β -carbofluoroethoxy-3 β -(4'-methyl-phenyl)nortropine) has faster kinetics compared with ^{11}C -PE2I [7, 9] and can therefore be a very suitable radioligand for clinical imaging of the entire nigrostriatal pathway and DAT quantification in PD patients. Its affinity for DAT is comparable with ^{123}I -FP-CIT ($K_i = 12$ nM) but selectivity is much better (PE2I affinity for serotonin transporter (SERT) and norepinephrine transporter (NET) is 29-fold and 58-fold lower, respectively, than for DAT) [7, 11].

As most brain regions outside the nigrostriatal pathway express little or no DAT, several cortical or cerebellar reference regions can be considered. The use of a dynamic simplified reference tissue model (SRTM) approach has already been validated by several authors for ^{18}F -FE-PE2I [7, 10, 12]. However, for clinical purposes, especially in an aged patient population, a shorter scan time and a simplified quantification protocol to improve patient tolerability are needed. Different approaches for static scanning of ^{18}F -FE-PE2I have been investigated, but no general agreement has been reached so far [5, 12, 13]. Sonni et al. found that the 16.5–42-min time window was optimal as $\text{SUVR}_{16.5-42}$ correlated best with BP_{ND} ($r^2 = 0.98$), despite an underestimation of the BP_{ND} [13]. Ikoma et al. concluded that the SUVR estimates in the 70–90-min time frame were stable and correlated well with the $\text{BP}_{2\text{CM}}$ ($r = 0.82-0.86$), although the $\text{BP}_{\text{SUVR}70-90}$ largely overestimated the $\text{BP}_{2\text{CM}}$ [12]. Jakobson et al. compared the diagnostic performance of ^{18}F -FE-PE2I PET with ^{123}I -FP-CIT SPECT and found that pseudoequilibrium was reached after 50 min for ^{18}F -FE-PE2I, and SUVR_{50-75} was selected as the optimal time window [5]. In these three studies, the cerebellum (CBL) was used as reference region, although cerebellar

time activity curves show slower kinetics than neocortical (e.g., occipital) regions [14]. For clinical DAT imaging using ^{123}I -FP-CIT, the occipital cortex (OC) is widely used as a reference region because it can be delineated and quantified in the same midtransverse planes as the striatum [15].

In view of the existing debate, the aim of this study was to define an optimal static time window and reference region for analysis of ^{18}F -FE-PE2I PET in a clinical setting, optimizing both correlation and bias with respect to SRTM-derived BP_{ND} as ground truth and propose a suitable time frame with optimal clinical applicability. In addition, we compared the discriminatory value and effect size for ^{18}F -FE-PE2I with that for ^{123}I -FP-CIT scan currently used in clinical practice, in a set of patients that underwent both investigations.

Materials and methods

Subject demographics (Tables 1 and 2)

For ^{18}F -FE-PE2I, healthy volunteers (HV) were prospectively recruited through website advertisements and local newspapers. Main exclusion criteria were abnormal findings on clinical (neurological or general physical) examination, history of important neurological or psychiatric disorders, and major internal pathology (diabetes, cancer, etc.). For ^{123}I -FP-CIT, 14 historical HV (58.1 ± 12.5 years, 5M) were used, which formed part of the European Normal Control Database (ENC-DAT) that were scanned in our center [16].

PD patients were prospectively recruited in the Movement Disorders Clinic of the University Hospitals Leuven. The diagnosis of PD was based on the UK Parkinson's Disease Society Brain Bank criteria. Exclusion criteria were a history of neurological or psychiatric diseases other than PD and major internal pathology. All PD patients had previously undergone a ^{123}I -FP-CIT scan as part of their diagnostic workup. Unified Parkinson's Disease Rating Scale (UPDRS), Hoehn-Yahr (HY) scale, and Mini Mental State Examination (MMSE) scores were determined on medication. Levodopa equivalent daily dose (LEDD) was calculated as described [17].

Written informed consent was given by every participant. This study was approved by the local university hospital Ethics Committee for Research and the study was performed in accordance to the World Medical Association Declaration of Helsinki. All subjects signed an informed consent form.

Data acquisition

All subjects underwent a 60-min dynamic ^{18}F -FE-PE2I PET-MR scan (GE Signa 3T PET-MR). For that, an activity of 144

Table 1 Demographic and clinical characteristics of study subjects. Total study group

	PD patients	HV (^{18}F -FE-PE2I)	HV (^{123}I -FP-CIT)	<i>p</i> value
Number	9	34	14	–
Age (years)	64.3 ± 6.8 (47–70)	47.7 ± 16.8 (18–79)	58.1 ± 12.5 (39–78)	0.106
Gender (M/F)	3/6	13/21	5/9	0.425
Disease duration (months)	18.2 ± 10.6	–	–	–
Handedness (R-L-B)	7-0-1	25-6-2	13-1-0	0.601
Hoehn and Yahr stage				–
1 (unilateral symptoms)	2	–	–	
2 (bilateral symptoms)	7	–	–	
UPDRS total	29.9 ± 15.5	4.6 ± 4.2	–	< 0.001
UPDRS part III	21.8 ± 10.0	2.1 ± 1.9	–	< 0.001
LEDD (mg)	225 ± 123	–	–	–
MMSE	29.1 ± 1.0	29.6 ± 0.6	–	0.218

Data are given as mean ± standard deviation

Numbers between brackets indicate range (min–max)

PD Parkinson's disease, HV healthy volunteers, M male, F female, R right, L left, B bimanual, UPDRS unified Parkinson's Disease Rating Scale, LEDD levodopa equivalent daily dose, MMSE Mini Mental State Examination

UPDRS was performed in 32 of 34 HV

MMSE scores were available for all 34 HV

± 18 MBq ^{18}F -FE-PE2I was administered. No arterial blood sampling or metabolite analysis was performed. All PD patients were on their standard dopaminergic medication.

PET data were collected in list mode and reconstructed using the following parameters (6×15 s, 3×30 s, 3×60 s, 3×180 s, 9×300 s) corrected for randoms, scatter, time-of-flight offset [18], and deadtime. Individual attenuation correction was performed using a validated in-house zero echo time (ZTE) approach [19]. Ordered Subsets Expectation Maximization (28 subsets with 4 iterations), including time-of-flight information, resolution modeling, and Gaussian postsMOOTHING with a Full-Width-at-Half-Maximum (FWHM) kernel of 4.5 mm (isotropic), was used for reconstruction.

Several simultaneous MR sequences were collected. For this study, we used the volumetric T1-weighted 3D BRAVO sequence (plane: sagittal; TE 3.2 ms; T4 8.5 ms; TI 450 ms; flip angle 12; receiver bandwidth 32; NEX 1).

For ^{123}I -FP-CIT scan, thyroid protection (1 ml of Lugol) prior to injection was administered, and an activity of 170 ± 22 MBq ^{123}I -FP-CIT was injected. ^{123}I -FP-CIT scans of the 14 HV were performed on an E.cam system (Siemens, Erlangen, Germany). Thirty-minute ^{123}I -FP-CIT scans of the 9 PD patients were performed on a GE Discovery 670 SPECT-CT (General Electric, Buc, France). As both groups were scanned on different dual-head cameras, reconstructions were performed offline with the same calculated attenuation correction (uniform attenuation 0.15/cm) to minimize scanner variance. Reconstructions were performed using iterative reconstruction with OSEM (5 iterations and 8 subsets, followed by 3

iterations with 4, 2, and 1 subsets, respectively), scatter correction (acquisition with dual energy window), and modeling of collimator blurring. Gaussian postsMOOTHING with a kernel of 7.5 mm FWHM was applied. The interval between ^{123}I -FP-CIT scan and ^{18}F -FE-PE2I scan in the 9 PD patients was 6.9 ± 3.8 months (range 1.6–13.0).

Data analysis

^{18}F -FE-PE2I

Motion correction was implemented with a rigid co-registration of each frame to the average of the first 12 frames representing the first 6 min of the PET acquisition. Spatial normalization to the MNI template was performed in PMOD (v3.7, PMOD technologies, Zurich, Switzerland) using the 3D T1 BRAVO and probability maps transformation restricted to the subject-specific gray matter part of the whole brain with a fixed threshold of 0.3. Cerebellar, occipital, striatal, and substantia nigra (SN) time activity curves (TACs) were calculated using the PNEURO tool with the Hammers atlas (N30R83). For the caudate nucleus (CAU) and putamen (PUT), the PMOD parcellation was used as this module allows improved subcortical VOI delineation. BP_{ND} (SRTM model) and SUVR images were calculated using both OC and CBL as reference regions. $\text{SUVR}_{[t_1-t_2]}$ images at three time intervals [t_1-t_2] (minutes postinjection (pi)) were investigated: [15–40], [40–60], and [50–60].

Table 2 Demographic and clinical characteristics of study subjects. Age- and gender-matched subgroup for [¹⁸F]-FE-PE2I

	PD patients	HV (¹⁸ F-FE-PE2I)	<i>p</i> value
Number	9	19	–
Age (years)	64.3 ± 6.8 (47–70)	60.1 ± 8.6 (49–79)	0.142
Gender (M/F)	3/6	5/14	0.921
UPDRS total	29.9 ± 15.5	1.9 ± 2.2	< 0.001
UPDRS part III	21.8 ± 10.0	4.2 ± 5.0	< 0.001
MMSE	29.1	29.6 ± 0.5	0.167

Data are given as mean ± standard deviation

Numbers between brackets indicate range (min–max)

PD Parkinson's disease, HV healthy volunteers, M male, F female, R right, L left, B bimanual, UPDRS unified Parkinson's Disease Rating Scale, LEDD levodopa equivalent daily dose, MMSE Mini Mental State Examination

UPDRS was performed in 32 of 34 HV

MMSE scores were available for all 34 HV

¹²³I-FP-CIT

Spatial normalization and VOI delineation (CAU left and right, PUT left and right, and OC) was performed in PMOD (v3.7) using the individual clinical T1-weighted MRI. The semi-quantitative uptake ratio (SUR) was calculated using the OC as reference region according to the following formula: (mean counts in each VOI)/(mean counts in OC).

General statistics

General statistics were calculated in SPSS (IBM Statistics v 25.0, IBM, NY, USA). For the Bland-Altman analysis, GraphPad Prism (GraphPad Software v5, San Diego, USA) was used.

The Spearman correlation coefficients for ¹⁸F-FE-PE2I were calculated between BP_{ND} + 1 and SUVR for CAU, PUT, and the ratio CAU/PUT (CPR). Similarly a Bland-Altman analysis was done for CAU, PUT, and CPR. The BP_{ND} + 1 was used as gold standard outcome measure. A discriminant analysis with leave-one-out approach was performed to discriminate between PD and HV using PUT and CPR. Additionally, Glass' effect size (Δ) using the HV group's standard deviation (SD), $\Delta = [(\text{mean}_{\text{HV}} - \text{mean}_{\text{PD}}) / \text{SD}_{\text{HV}}]$, was determined to compare the ability of the different time windows, different regions, and both tracers to differentiate between PD patients and HV.

A Mann-Whitney *U* test was used for group differences between PD and HV for both ¹⁸F-FE-PE2I SUVR and ¹²³I-FP-CIT SUR images with application of the exact significance option. Correlations between ¹⁸F-FE-PE2I SUVR_{50–60,occipital} and ¹²³I-FP-CIT SUR and percentage decrease for CAU and PUT compared with HV were determined using the Spearman correlation coefficients.

For all analyses, unilateral values for CAU, PUT, and CPR were used. For HV, we used the left-sided value for CAU, PUT, and CPR. For PD patients with lateralized symptoms (strictly unilateral or bilateral with asymmetry), the value contralateral to the clinically most affected side was used. If the patients had symmetrical symptoms, the left side was chosen.

Results

Demographics and parametric images

Nine PD patients for ¹⁸F-FE-PE2I and ¹²³I-FP-CIT, 34 HV for ¹⁸F-FE-PE2I, and 14 HV for ¹²³I-FP-CIT were included. Tables 1 and 2 show the demographic variables and clinical parameters for the three groups. Kinetic optimization was performed on all ¹⁸F-FE-PE2I scans. For comparison of ¹⁸F-FE-PE2I between PD and HV, an age- and gender-matched subgroup of ¹⁸F-FE-PE2I HV was used (Table 2).

All 9 ¹⁸F-FE-PE2I and ¹²³I-FP-CIT scans of the PD patients were visually abnormal. Figure 1 shows a typical ¹⁸F-FE-PE2I example of midtransverse slices for BP_{ND} and the various SUVR_[1–2] parametric images for both a PD patient and a HV. An example of ¹⁸F-FE-PE2I and ¹²³I-FP-CIT for a PD patient and HV is illustrated in Fig. 2.

Optimal time window and reference region selection for ¹⁸F-FE-PE2I

The Bland-Altman plots of CAU, PUT, and CPR separately for the different time windows and reference regions are shown in Fig. 3. Biases for CAU, PUT, and CPR are reported in Table 3. For CAU and PUT, the absolute value of the bias was generally smaller for PD patients compared with HV. In contrast, CPR biases were smaller for HV than for PD patients. The bias was overall smaller when OC was used as reference region compared with CBL.

Looking at the different time intervals, the smallest absolute values of the bias was found for the [15–40] interval, with the exception of CPR in HV where most late time windows had a smaller bias. Bias for CPR was overall small (0.193 or smaller). The bias for CAU, PUT, and CPR was mainly negative for the two late time intervals due to an average overestimation of BP_{ND} + 1.

Correlations between BP_{ND} + 1 and SUVR for the different time windows are shown per reference region in Fig. 4. For CAU, PUT, and CPR, we found highly significant correlations ($\rho > 0.71$, $p < 0.001$) between BP_{ND} + 1 and SUVR values for all three time windows and both reference regions. However, the correlation for the [15–40] (range ρ [0.71–0.90]) was lower than for the [40–60] (range ρ [0.88–0.94]) and the [50–60]-min (range ρ [0.91–0.96]) time interval. For all regions

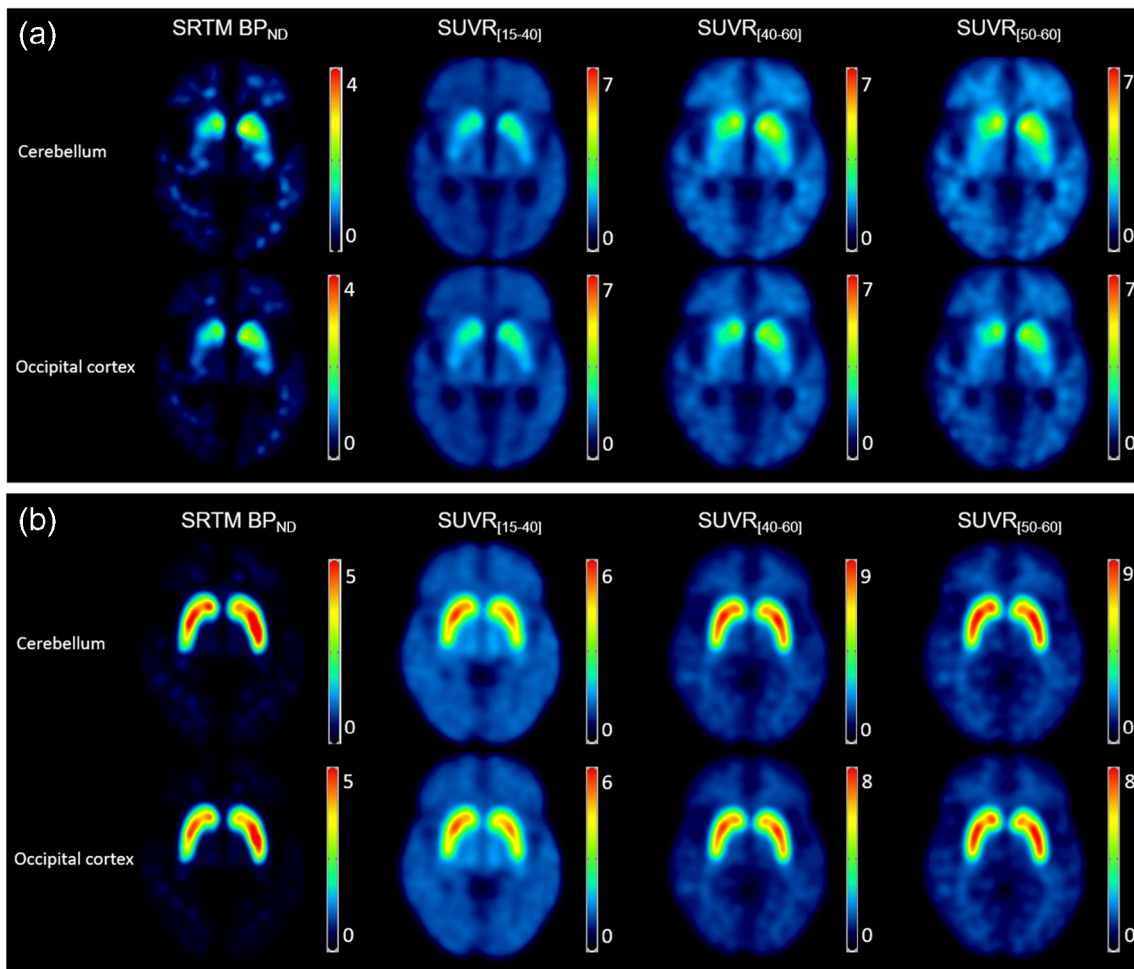


Fig. 1 Midtransverse ¹⁸F-FE-PE2I BP_{ND} and SUVR parametric images, for all 3 time windows and both reference regions. **a** Images of a Parkinson's disease (PD) patient (M, age 67 years, UPDRS mot = 23,

HY = 2). **b A healthy volunteer (HV) (F, age 52 years, UPDRS mot = 3). M, male; y, years; UPDRS III, UPDRS part III; HY, Hoehn and Yahr stage**

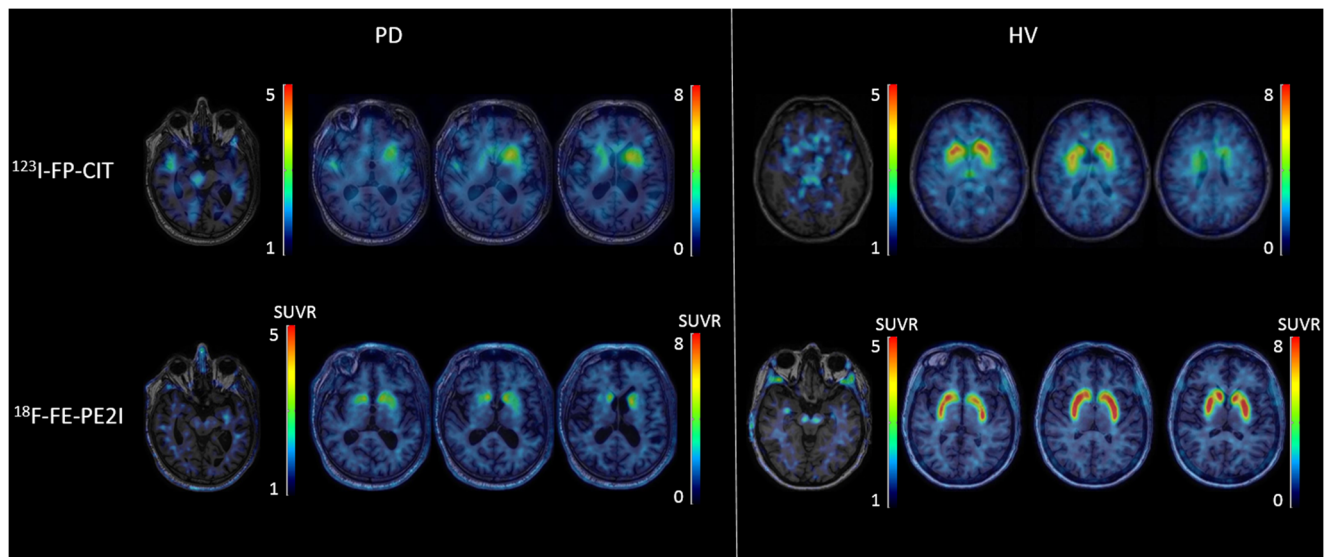


Fig. 2 ¹²³I-FP-CIT (upper row) and ¹⁸F-FE-PE2I (lower row) images of a 67-year-old Parkinson's disease (PD) patient (Hoehn and Yahr 2) and healthy volunteers (HV) (45 years old for ¹²³I-FP-CIT, 52 years old for

¹⁸F-FE-PE2I). Images in radiological orientation. The red arrow points to the uptake in the substantia nigra

(a) Cerebellum as reference region.

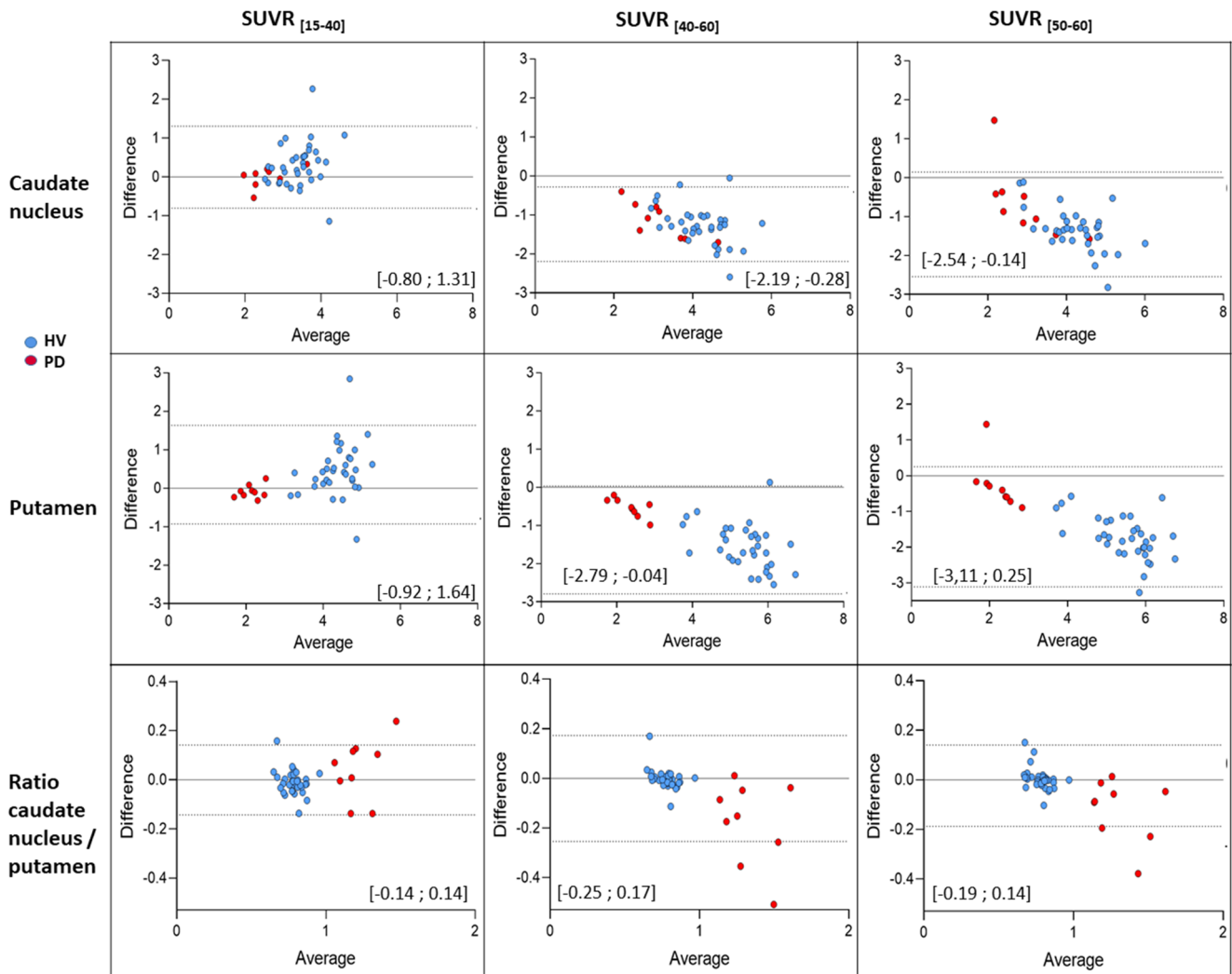


Fig. 3 Result of the Bland-Altman analysis ^{18}F -FE-PE2I: bias or mean difference between $\text{BP}_{\text{ND}} + 1$ and SUVR in different time windows for patients with Parkinson's disease (PD) ($n = 9$) and healthy volunteers

(HV) ($n = 34$). Dotted lines show the upper and lower 95% limit of agreement; values are shown between brackets. **a** Cerebellum as reference region. **b** Occipital cortex as reference region

and all time windows, the correlation was equal or higher with the OC as reference region compared with the CBL.

Group differences and discriminant analysis between PD patients and age-matched HV using ^{18}F -FE-PE2I and ^{123}I -FP-CIT

The boxplot of the $\text{SUVR}_{[t1-t2]}$ values for the PD patients and HV for every time window is shown in Fig. 5. The effect sizes were 4.1 for the early time window, 4.1 for the intermediate time window, and 3.9 for the late time window for OC, and 3.8, 3.7, and 3.9 for CBL, respectively.

The results of the discriminant analysis are shown in Table 4. All time frame windows and both the PUT and CPR resulted in high discriminative power of more than

90%. Accuracy was identical or higher using the OC as reference region.

The Mann-Whitney U test showed a significant difference between PD and HV using both tracers for the CAU ($p = 0.002$ for ^{18}F -FE-PE2I and $p = 0.002$ for ^{123}I -FP-CIT) and PUT ($p < 0.001$ for ^{18}F -FE-PE2I and $p = 0.001$ for ^{123}I -FP-CIT). CPR was only significantly different for ^{18}F -FE-PE2I ($p < 0.001$). Effect sizes were 1.5, 3.9, and -13.2 for the CAU, PUT, and CPR with ^{18}F -FE-PE2I, and 1.5, 1.7, and -0.4 for the CAU, PUT, and CPR with ^{123}I -FP-CIT (Table 5). The percentage DAT decrease in PD patients was $22.0 \pm 16.6\%$ for CAU and $59.4 \pm 6.7\%$ for PUT with ^{18}F -FE-PE2I $\text{SUVR}_{50-60, \text{occipital}}$, and $22.7 \pm 12.4\%$ for CAU and $33.4 \pm 10.2\%$ for PUT with ^{123}I -FP-CIT SUR (Fig. 6). In addition, ^{18}F -FE-PE2I, unlike ^{123}I -FP-CIT, allowed

(b) Occipital cortex as reference region.

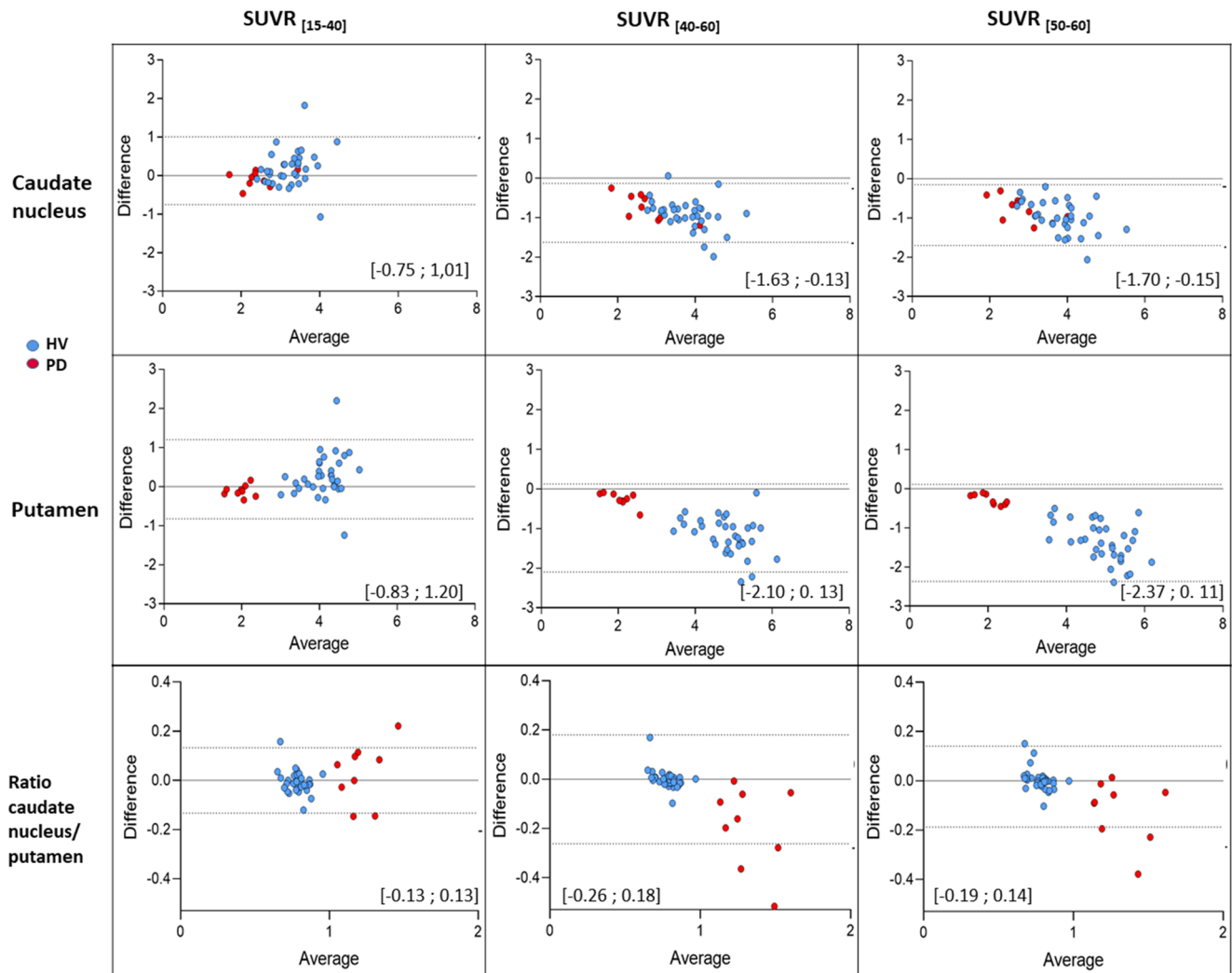


Fig. 3 (continued)

measurement of DAT levels in the SN. ¹⁸F-FE-PE2I showed a decrease for SN of 17.3 ± 8.6% in PD compared with HV, with an effect size of 1.7 (Fig. 6c).

¹⁸F-FE-PE2I SUVR_{50-60,occipital} and ¹²³I-FP-CIT SUR for CAU and PUT were significantly correlated with $\rho = 0.87$ ($p = 0.002$), 0.88 ($p = 0.002$), and 0.92 ($p < 0.001$).

Table 3 Result of the Bland-Altman analysis (¹⁸F-FE-PE2I) for the different time windows and both reference regions in Parkinson’s disease (PD) patients compared w healthy volunteers (HV). Values are shown for caudate nucleus (CAU), putamen (PUT) and ratio caudate nucleus/putamen (CPR)

	15–40		40–60		50–60	
	PD	HV	PD	HV	PD	HV
CAU						
Cerebellum	-0.019	0.322	-1.135	-1.264	-0.660	-1.344
Occipital cortex	-0.085	0.184	-0.736	-0.918	-0.744	-0.975
PUT						
Cerebellum	-0.090	0.471	-0.534	-1.603	-0.272	-1.738
Occipital cortex	-0.115	0.269	-0.259	-1.178	-0.277	-1.357
CPR						
Cerebellum	0.043	-0.012	-0.179	-0.004	-0.121	0.002
Occipital cortex	0.028	-0.008	-0.193	-0.001	-0.193	0.014

(a) Cerebellum as reference region.

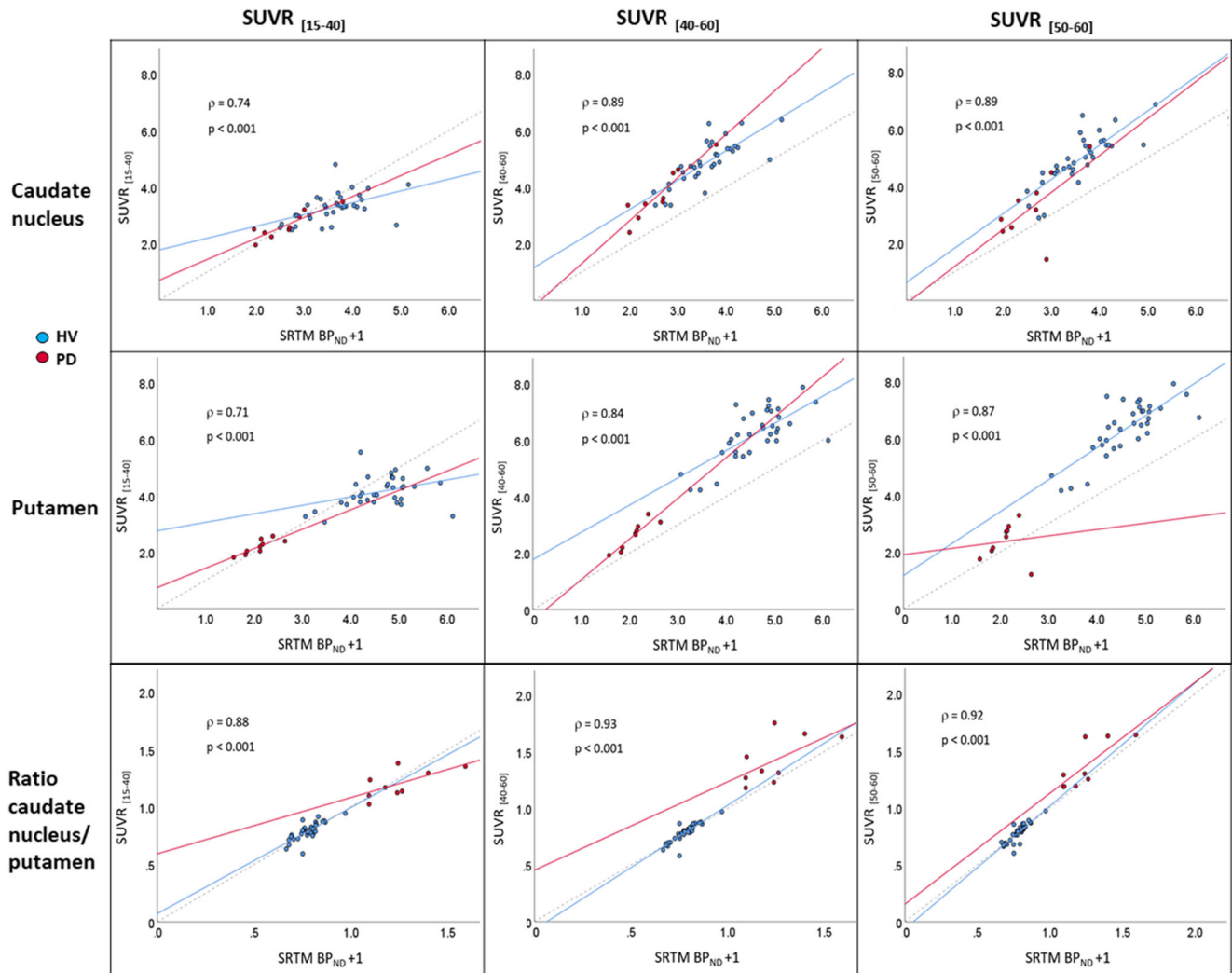


Fig. 4 Correlation (Spearman) between ^{18}F -FE-PE2I $\text{BP}_{\text{ND}} + 1$ and SUVR, for each time window and reference region for patients with Parkinson's disease (PD) ($n = 9$) and healthy volunteers (HV) ($n = 34$).

Dotted line shows line of identity. **a** Cerebellum as reference region. **b** Occipital cortex as reference region

The percentage decrease in PD compared with HV with ^{18}F -FE-PE2I and ^{123}I -FP-CIT for the CAU and PUT were also significantly correlated, with $\rho = 0.87$ ($p = 0.002$) and 0.88 ($p = 0.002$), respectively, as shown in Fig. 7. In the PD group, no correlation was observed between motor UPDRS scores and either ^{18}F -FE-PE2I or ^{123}I -FP-CIT uptake.

Discussion

^{18}F -FE-PE2I-PET has been shown to be an excellent imaging tool for in vivo DAT quantification in the entire nigrostriatal tract [1, 7, 10]. However, some discussion exists about the optimal reference region and time

window. Therefore, in the present study, we aimed to define the optimal static scanning protocol for clinical applications.

Until now, only the CBL has been used as a reference region for ^{18}F -FE-PE2I-PET scans. However, Odano et al. showed that the CBL has slower kinetics compared with the OC, suggesting that a cortical region (e.g., OC) may be better suited as a reference region. Additionally, the OC is situated in the same transversal plane as the striatum, which facilitates delineation. Moreover, the OC is also utilized as reference region for clinical ^{123}I -FP-CIT-SPECT DAT scans. Therefore, we performed a head-to-head comparison between CBL and OC as reference regions. Our results demonstrated smaller bias, higher correlations, and identical or higher discriminative power using OC for all time windows. Therefore,

(b) Occipital cortex as reference region.

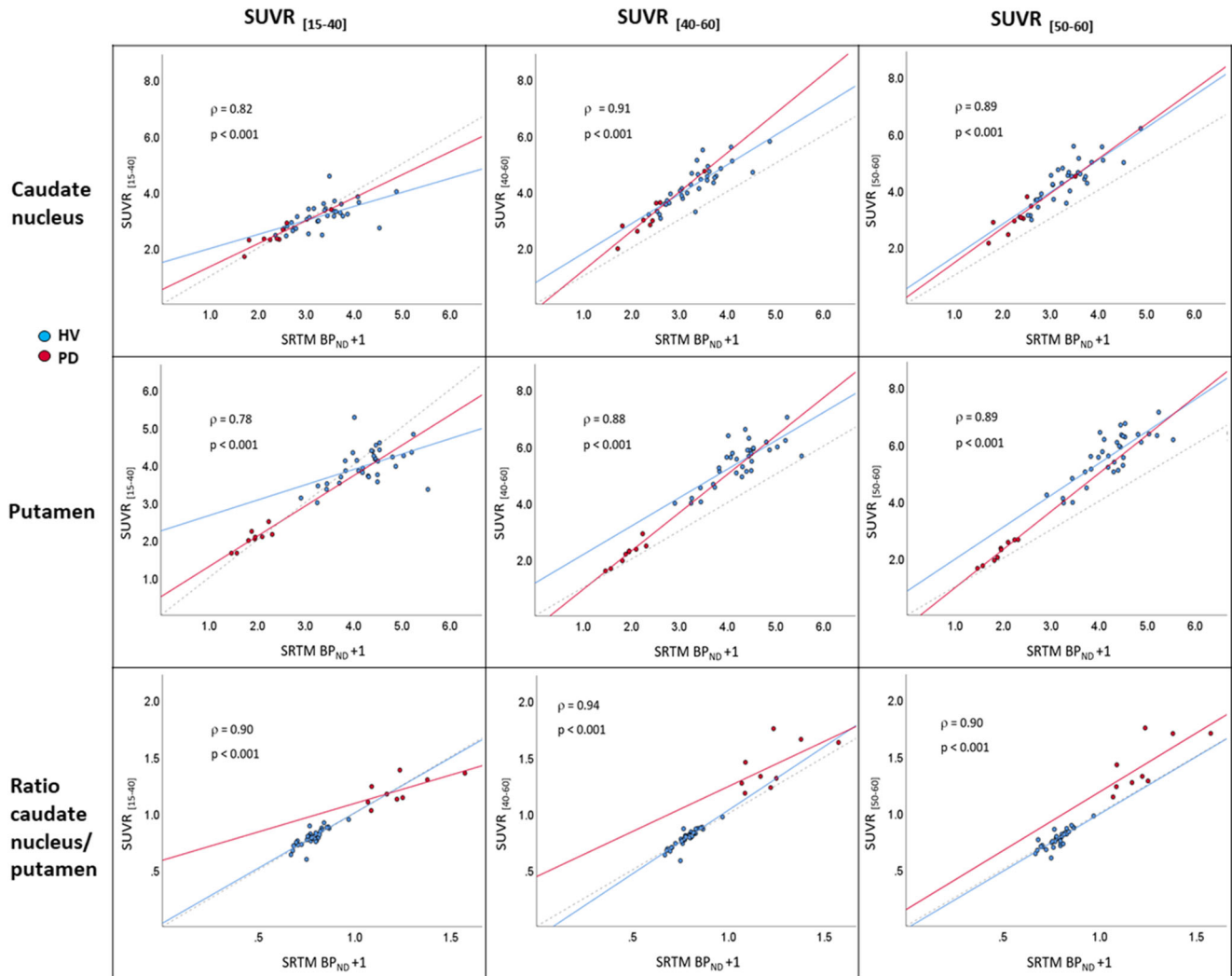


Fig. 4 (continued)

in future studies, the OC should be considered as the reference region for ¹⁸F-FE-PE2I-PET scans instead of the CBL.

In contrast to some research purposes where closeness to BP_{ND} as gold standard is the key, discriminative power and clinical feasibility are most important for clinical practice. Therefore, we compared the three time windows in terms of quantification, discriminative power, and clinical feasibility.

First, we looked at the quantification. Overall, the smallest bias was observed with the [15–40] time window compared with the late time windows. However, the correlation between BP_{ND} + 1 and SUVR was slightly better for the late time windows compared with [15–40]. Therefore, for absolute quantification, the early time window seems more optimal as bias was substantially smaller with only a slight decrease in correlation.

Second, we performed a discriminant analysis to determine the respective discriminative power. The discriminant analysis for the PUT and CPR between the PD patients and HV

resulted in high sensitivity, high specificity, and high accuracy using all time windows and both reference regions. Effect sizes were similar for all three time windows. In conclusion, all time windows are able to distinguish between PD and HV.

Finally, we addressed the clinical feasibility. Scan length is of critical importance especially in patients with neurodegenerative diseases such as PD. Long acquisition may result in substantial discomfort for this vulnerable patient population. Also, unexpected practical issues may disturb the suggested time schedule. Therefore, the shortest possible acquisition time window during pseudoequilibrium is preferred for clinical use. Likewise, for the current clinical standard, ¹²³I-FP-CIT SPECT, scanning is performed 3 to 6 h pi when pseudoequilibrium is reached. For ¹⁸F-FE-PE2I-PET, pseudoequilibrium is reached at 50 min pi, reducing the waiting time significantly compared with ¹²³I-FP-CIT SPECT. Moreover, our data showed that a short 10-min static scan appeared to be sufficient for clinical practice.

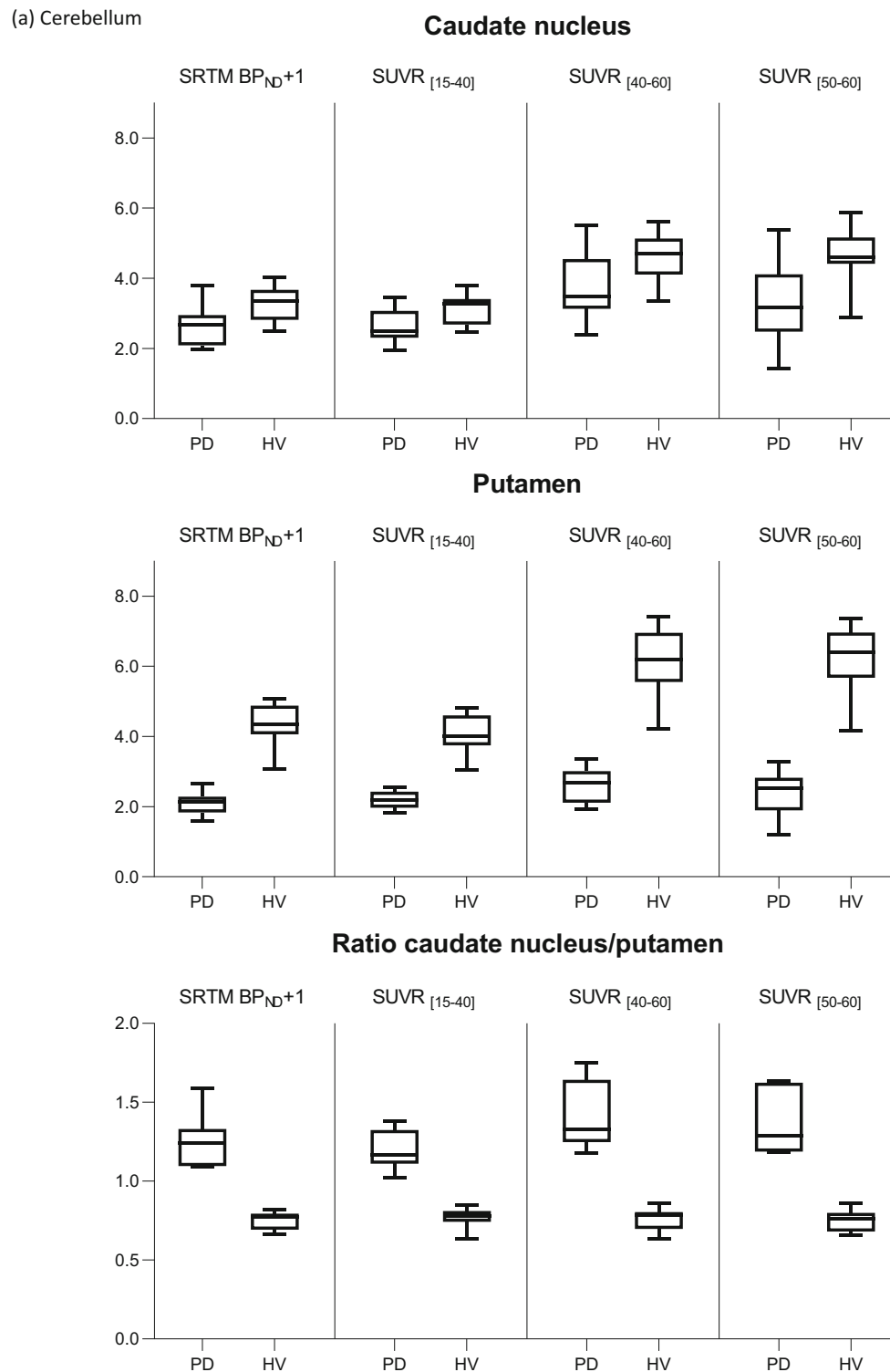


Fig. 5. Boxplot of ^{18}F -FE-PE2I $\text{SUVR}_{[t_1-t_2]}$ and $\text{BP}_{ND} + 1$ of putamen, caudate nucleus, and ratio caudate nucleus/putamen, for reference regions cerebellum and occipital cortex, in patients with Parkinson's disease (PD) ($n = 9$) and healthy volunteers (HV) ($n = 19$). **a** Cerebellum. **b** Occipital cortex

(b) Occipital

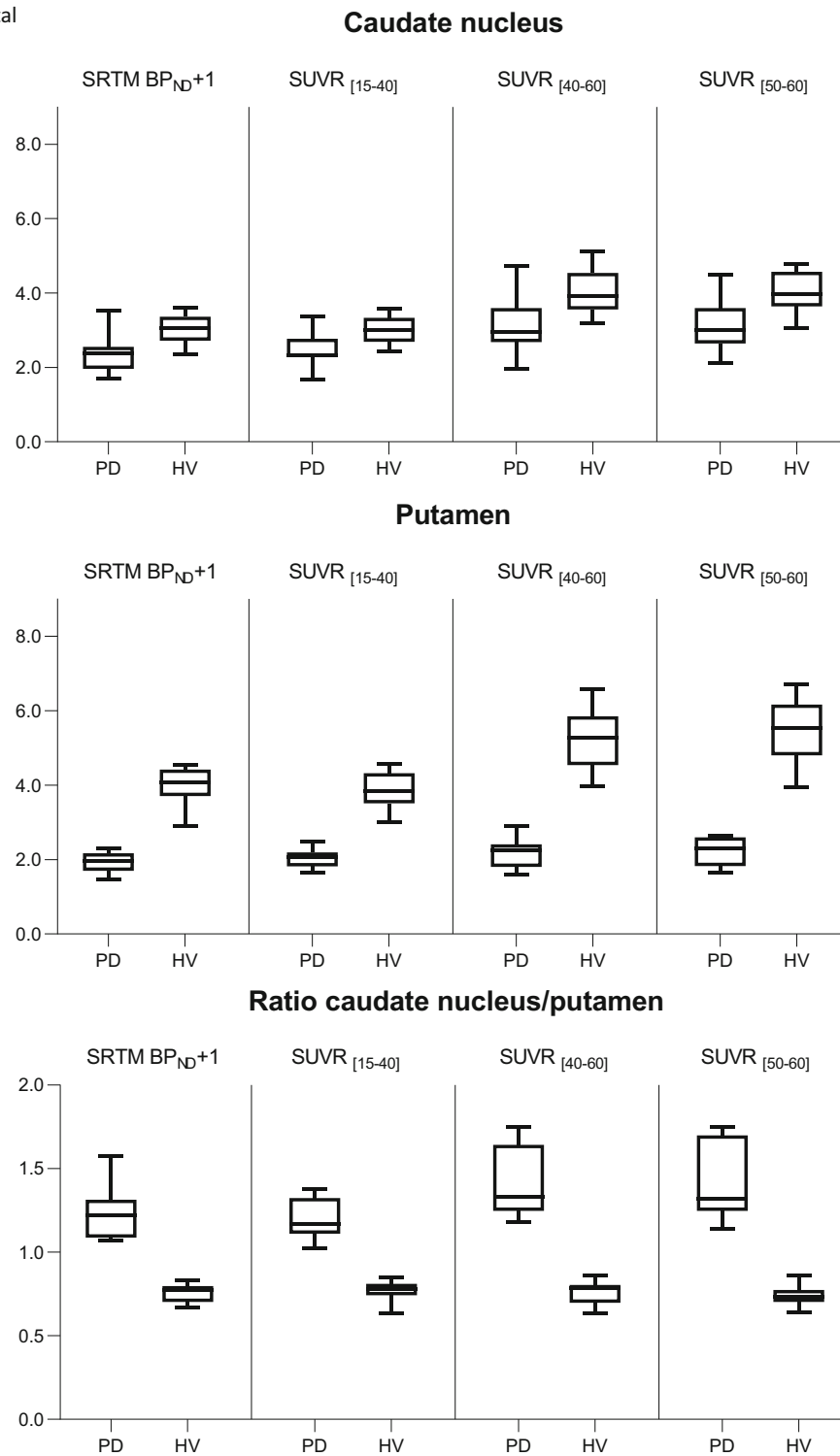


Fig. 5 (continued)

Table 4 ^{18}F -FE-PE2I and ^{123}I -FP-CIT discriminant analyses using the leave-one-out approach using the putamen (PUT) and the ratio caudate nucleus/putamen (CPR)

	Putamen				Ratio caudate nucleus/putamen			
	SUVR _[15–40]	SUVR _[40–60]	SUVR _[50–60]	BP _{ND} + 1	SUVR _[15–40]	SUVR _[40–60]	SUVR _[50–60]	BP _{ND} + 1
Cerebellum (^{18}F -FE-PE2I)								
Sensitivity	1.00	1.00	1.00	1.00	1.00	1.00	1.00	1.00
Specificity	0.95	0.89	0.89	0.95	1.00	1.00	1.00	1.00
Accuracy	0.96	0.93	0.93	0.93	1.00	1.00	1.00	1.00
Occipital cortex (^{18}F -FE-PE2I)								
Sensitivity	1.00	1.00	1.00	1.00	1.00	1.00	1.00	1.00
Specificity	1.00	1.00	1.00	1.00	1.00	1.00	1.00	1.00
Accuracy	1.00	1.00	1.00	1.00	1.00	1.00	1.00	1.00
Occipital cortex (^{123}I -FP-CIT)								
	Putamen				Ratio caudate nucleus/putamen			
	Semi-quantitative uptake ratio				Semi-quantitative uptake ratio			
Sensitivity	0.89				0.78			
Specificity	0.79				0.64			
Accuracy	0.83				0.70			

The correlation in binding potential and binding ratios between the two tracers was high, and the discriminatory value between healthy volunteers and patients was similar which is in line with the findings by Jakobson et al. [5]. Furthermore, effect sizes of PUT and CPR values between patients and controls for ^{18}F -FE-PE2I were substantially higher, which is due to the combination of a higher dynamic range for ^{18}F -FE-PE2I in striatal abnormalities in patients (the percentage DAT decrease measured by ^{18}F -FE-PE2I was approximately 60% compared with 30% for ^{123}I -FP-CIT) as well as lower intersubject variability. Both can be due to better imaging statistics per VOI and better spatial resolution with lower partial volume effects. It can therefore be reasonably assumed that, also in a clinical population of uncertain Parkinsonism, ^{18}F -FE-PE2I will be able to discriminate larger differences between patients with neurodegenerative Parkinsonism versus conditions without nigrostriatal DAT involvement such as essential tremor, psychogenic, or drug induced Parkinsonism.

In conclusion, our results suggest to scan early, 15 to 40 min pi, in case absolute quantification is the main aim. For clinical practice the [50–60] time frame seems most optimal both in terms of accuracy and clinical feasibility.

There are some limitations to our study. First, we had a relatively small patient group (9 PD patients). Nevertheless, even with 9 patients, good effect sizes were obtained. Second, the dynamic scan was acquired during 60 min; therefore, our late time frame during pseudoequilibrium lasted only 10 min which may have caused lower signal to noise. However, even with a 10-min time frame, we obtained similar discriminative power compared with the other time windows. Finally, our study only enrolled patients with an established clinical diagnosis of PD. Patients with unclear Parkinsonism were not included. Therefore, conclusions about clinical usefulness of ^{18}F -FE-PE2I needs to be verified in a clinically representative sample of patients with uncertain Parkinsonism.

Table 5 Comparison of ^{18}F -FE-PE2I (in SUVR_[50–60]) and ^{123}I -FP-CIT (in semi-quantitative uptake ratio) effect sizes (both with the occipital cortex as reference region)

	CAU		PUT		CPR	
	^{18}F -FE-PE2I	^{123}I -FP-CIT	^{18}F -FE-PE2I	^{123}I -FP-CIT	^{18}F -FE-PE2I	^{123}I -FP-CIT
Mean PD	3.12	2.99	2.20	2.79	1.42	1.07
Mean HV	4.00	3.87	5.42	4.19	0.74	0.96
SD HV	0.57	0.58	0.83	0.82	0.05	0.26
Effect size	1.55	1.51	3.88	1.72	– 13.2	– 0.41

CAU caudate nucleus, PUT putamen, CPR ratio caudate nucleus/putamen, PD Parkinson's disease patients, HV healthy volunteers, SD standard deviation

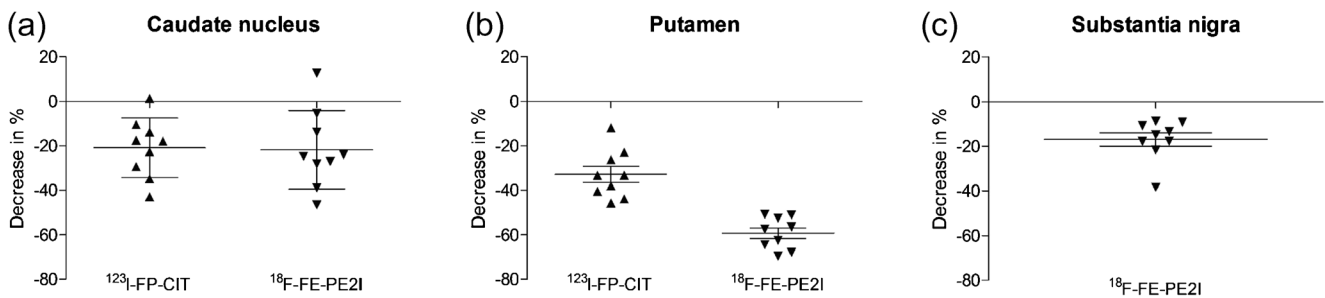


Fig. 6 Percentage decrease of $^{123}\text{I-FP-CIT}$ semi-quantitative uptake ratio and $^{18}\text{F-FE-PE2I}$ standardized uptake value (50–60 min post-injection, occipital cortex as pseudoreference region) in Parkinson’s disease patients compared with healthy volunteers in the caudate nucleus (a), putamen (b), and substantia nigra (c)

Conclusion

OC as reference region seems preferable over CBL because of the higher time stability, higher correlation of SUVR with $\text{BP}_{\text{ND}} + 1$, and lower bias. Of the three time frames, [15–40]

shows the lowest bias and may therefore be the optimal time window for quantification studies. For clinical use, [50–60] seems more optimal as correlations of SUVR with $\text{BP}_{\text{ND}} + 1$ are higher and pseudoequilibrium is reached. Direct comparison in patients with PD shows higher differences between

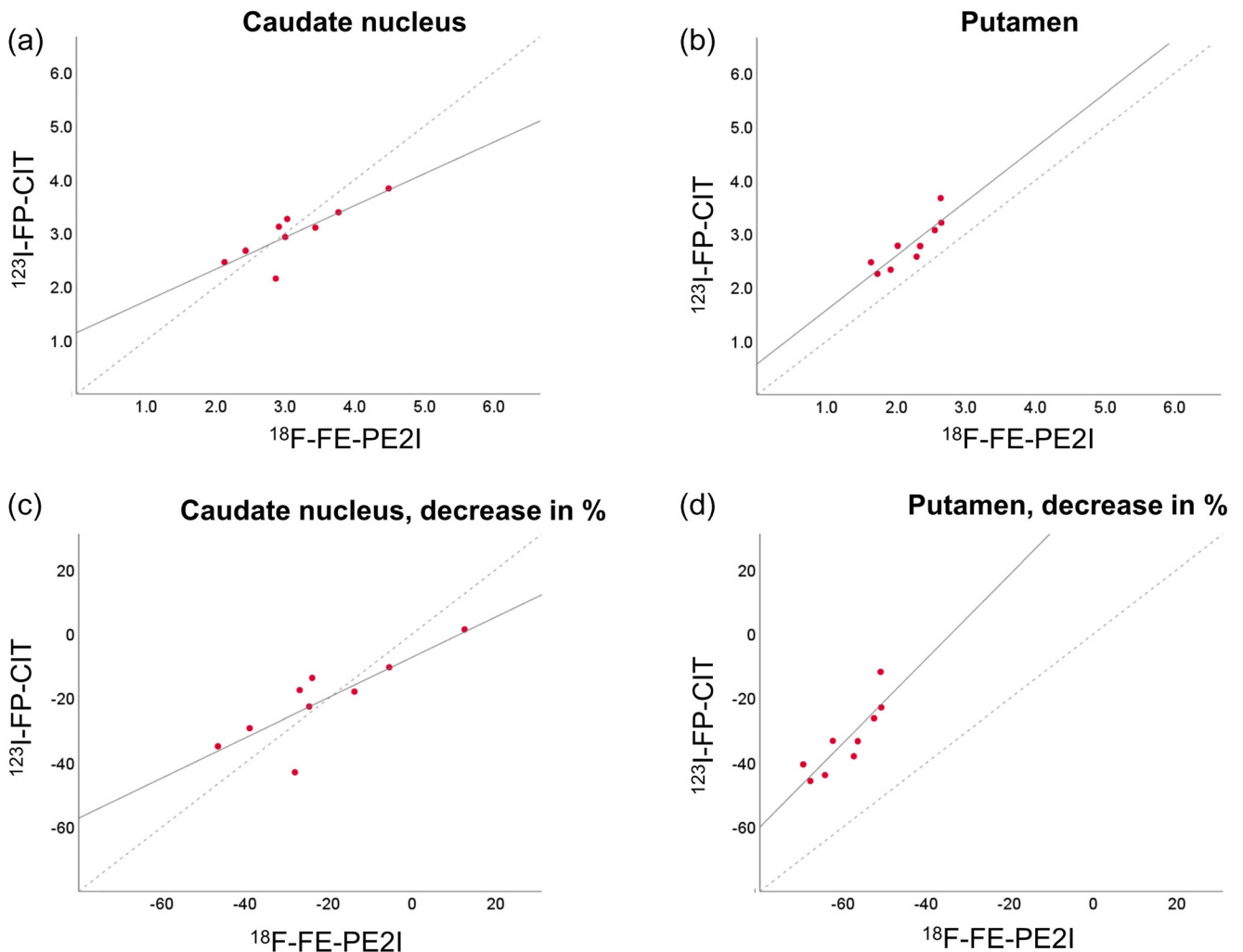


Fig. 7 Correlation between $^{123}\text{I-FP-CIT}$ and $^{18}\text{F-FE-PE2I}$ uptake in the caudate nucleus (a) and putamen (b) and between the percentage decrease in $^{123}\text{I-FP-CIT}$ and $^{18}\text{F-FE-PE2I}$ uptake in the caudate nucleus (c) and putamen (d) for the PD patients

patients and controls as well as larger effect sizes, thereby suggesting at least non-inferiority of ^{18}F -FE-PE2I compared with ^{123}I -FP-CIT.

Acknowledgments The authors explicitly want to thank Mr. Kwinten Porters and Mr. Jef Van Loock for their contributions to the scanning and data handling, and the PET radiopharmacy and medical physics teams of UZ Leuven for their skilled contributions.

Compliance with ethical standards

Conflict of interest Koen Van Laere and Wim Vandenberghe are Senior Clinical Investigators of the Fund for Scientific Research, Flanders, Belgium (FWO). Donatienne Van Weehaeghe and Aline Delva are PhD fellows of the FWO. Jenny Ceccarini is a postdoctoral fellow of the FWO. There are no other conflicts of interest.

Ethical approval All procedures performed in studies involving human participants were in accordance with the ethical standards of the institutional and/or national research committee (UZ/KU Leuven Ethical Committee Belgium) and with the 1964 Helsinki declaration and its later amendments or comparable ethical standards.

Informed consent Informed consent was obtained from all individual participants included in the study.

References

- Fazio P, Svenningsson P, Cselenyi Z, Halldin C, Farde L, Varrone A. Nigrostriatal dopamine transporter availability in early Parkinson's disease. *Mov Disord.* 2018;33(4):592–9.
- Uhl GR. Dopamine transporter: basic science and human variation of a key molecule for dopaminergic function, locomotion, and Parkinsonism. *Mov Disord.* 2003;18(Suppl 7):S71–80.
- Poewe W, Seppi K, Tanner CM, Halliday GM, Brundin P, Volkman J, et al. Parkinson disease. *Nat Rev Dis Primers.* 2017;3:17013.
- Brooks DJ. Molecular imaging of dopamine transporters. *Ageing Res Rev.* 2016;30:114–21.
- Jakobson Mo S, Axelsson J, Jonasson L, Larsson A, Ogren MJ, Ogren M, et al. Dopamine transporter imaging with [(18)F]FE-PE2I PET and [(123)I]FP-CIT SPECT—a clinical comparison. *EJNMMI Res.* 2018;8(1):100.
- Rahmim A, Zaidi H. PET versus SPECT: strengths, limitations and challenges. *Nucl Med Commun.* 2008;29(3):193–207.
- Sasaki T, Ito H, Kimura Y, Arakawa R, Takano H, Seki C, et al. Quantification of dopamine transporter in human brain using PET with 18F-FE-PE2I. *J Nucl Med.* 2012;53(7):1065–73.
- Varrone A, Halldin C. New developments of dopaminergic imaging in Parkinson's disease. *Q J Nucl Med Mol Imaging.* 2012;56(1):68–82.
- Varrone A, Toth M, Steiger C, Takano A, Guilloteau D, Ichise M, et al. Kinetic analysis and quantification of the dopamine transporter in the nonhuman primate brain with 11C-PE2I and 18F-FE-PE2I. *J Nucl Med.* 2010;52(1):132–9.
- Fazio P, Svenningsson P, Forsberg A, Jonsson EG, Amini N, Nakao R, et al. Quantitative analysis of (1)(8)F-(E)-N-(3-iodoprop-2-enyl)-2beta-carbofluoroethoxy-3beta-(4'-methyl-phenyl) nortropine binding to the dopamine transporter in Parkinson disease. *J Nucl Med.* 2015;56(5):714–20.
- Pinborg LH, Ziebell M, Frokjaer VG, de Nijs R, Svarer C, Haugbol S, et al. Quantification of 123I-PE2I binding to dopamine transporter with SPECT after bolus and bolus/infusion. *J Nucl Med.* 2005;46(7):1119–27.
- Ikoma Y, Sasaki T, Kimura Y, Seki C, Okubo Y, Suhara T, et al. Evaluation of semi-quantitative method for quantification of dopamine transporter in human PET study with (1)(8)F-FE-PE2I. *Ann Nucl Med.* 2015;29(8):697–708.
- Sonni I, Fazio P, Schain M, Halldin C, Svenningsson P, Farde L, et al. Optimal acquisition time window and simplified quantification of dopamine transporter availability using 18F-FE-PE2I in healthy controls and Parkinson disease patients. *J Nucl Med.* 2016;57(10):1529–34.
- Odano I, Varrone A, Hosoya T, Sakaguchi K, Gulyas B, Padmanabhan P, et al. Simplified estimation of binding parameters based on image-derived reference tissue models for dopamine transporter bindings in nonhuman primates using [(18)F]FE-PE2I and PET. *Am J Nucl Med Mol Imaging.* 2017;7(6):246–54.
- Vermeulen RJ, Wolters EC, Tissingh G, Booij J, Janssen AG, Habraken J, et al. Evaluation of [123I] beta-CIT binding with SPECT in controls, early and late Parkinson's disease. *Nucl Med Biol.* 1995;22(8):985–91.
- Varrone A, Dickson JC, Tossici-Bolt L, Sera T, Asenbaum S, Booij J, et al. European multicentre database of healthy controls for [123I]FP-CIT SPECT (ENC-DAT): age-related effects, gender differences and evaluation of different methods of analysis. *Eur J Nucl Med Mol Imaging.* 2013;40(2):213–27.
- Tomlinson CL, Stowe R, Patel S, Rick C, Gray R, Clarke CE. Systematic review of levodopa dose equivalency reporting in Parkinson's disease. *Mov Disord.* 2010;25(15):2649–53.
- Rezaei A, Schramm G, Van Laere K, Nuyts J. Estimation of crystal timing properties and efficiencies for the improvement of (joint) maximum-likelihood reconstructions in TOF-PET. *IEEE Trans Med Imaging.* 2019.
- Schramm G, Koole M, Willekens S, Ahmadreza R, Van Weehaeghe D, Delso G et al. Regional accuracy of ZTE-based attenuation correction in static and dynamic brain PET/MR. *Medical Physics.* 2018.

Publisher's note Springer Nature remains neutral with regard to jurisdictional claims in published maps and institutional affiliations.